

# Low-loss 1310nm/1550nm Integrated Silicon Duplexer based on a Directional Coupler

Daivid Fowler<sup>1</sup>, Bertrand Szelag<sup>1</sup>, Vincent Hugues<sup>1</sup>, Christian Sillans<sup>2</sup>,  
Stéphane Bernabé<sup>1</sup> and Christophe Kopp<sup>1</sup>

<sup>1</sup>Univ. Grenoble Alpes, CEA, LETI, MINATEC campus, F38054 Grenoble, France

<sup>2</sup>IFOTEC, ZAC de Champfeuillet, Route des Bois, 38500 Voiron, France

**Keywords:** Silicon Photonics, Photonic Integrated Circuits, Passive Components, Multiplexer, Duplexer.

**Abstract:** We describe the design, fabrication and measurement of an integrated silicon photonics O-band/C-band duplexer. The duplexer is based on a directional coupler and is designed to be polarisation insensitive at 1550nm in order to be used in conjunction with a broadband integrated edge coupler. The measured insertion losses are <1.3dB with a -1dB bandwidth of ~80nm.

## 1 INTRODUCTION

The increasing maturity of integrated silicon photonics technology means that it is becoming increasingly attractive to substitute traditional discrete optical componentry with a low cost integrated solution. Here, we report the design, fabrication and measurement of a 1310/1550nm duplexer for use in bi-directional high-bitrate single-fiber systems, which is relevant for 1000BASE-BX10 and FTTH.

The use of integrated silicon photonics in this type of application could lead to significant cost reductions by eliminating many of the precise mechanical operations involved in the assembly of discrete optical components, leaving only the attachment of the fiber to the integrated source-detector-duplexer. This potentially decreases the module costs by a significant margin.

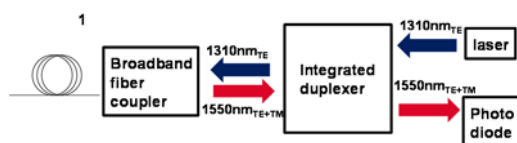


Figure 1: Typical circuit schematic for a 1000BASE-BX10 type gigabit Ethernet module.

Figure 1 shows a schematic of the circuit considered here. A modulated source laser operating at 1310nm passes through a duplexer before leaving downstream on a single mode fibre via a broadband

fibre coupler. Incoming, upstream data arrives in the same fibre, using a modulated 1550nm signal. The state of polarisation of the incoming light from the network is intrinsically unknown and unstable. This light will then be transferred into a combination of TE and TM modes in the on-chip waveguide via the broadband edge-type fibre coupler (Vivien *et al*, 2009). While integrated germanium photodiodes (Cardenas *et al*, 2014) are largely insensitive to the polarisation state in the incoming waveguide, photonic circuit waveguides tend to be designed in order to avoid unwanted crosstalk between polarisation states, and therefore have unequal refractive index values for TM and TE modes. Therefore, care must be taken that the duplexer not only splits/combines 1310/1550nm light, but also exhibits low polarisation dependent loss for the 1550nm light.

## 2 DESIGN

Silicon photonics devices for multiplexing have been widely developed to address single-band operation (e.g. DWDM or CWDM) (Okamoto, 2014), however, these solutions are not necessarily appropriate for inter-band applications. Such duplexing devices have been demonstrated on a silicon platform using diffractive gratings (Roelkens, 2007), the multimode interference effect (Hong and Lee 2007) and planar reflective gratings (S. Bidnyk *et al*, 2007). Here we

describe the use of a directional coupler to obtain very low (<1dB) insertion losses.

Directional couplers are based on the transfer of an optical field between two identical adjacent waveguides via the coupling of evanescent modes. They are often used in photonic circuits as a low-loss component to separate the optical field in a single waveguide into two waveguides with a pre-selected intensity ratio. If a first waveguide carrying an optical mode with a power,  $P_1$ , runs parallel to a second waveguide, the amount of transmitted power,  $P_2$ , is given by

$$P_2 = P_1 \sin^2(\pi L \delta n_{eff} / \lambda), \quad (1)$$

where  $L$  is the length of the parallel waveguides,  $\lambda$  is the operating wavelength and  $\delta n_{eff}$  is the difference between the symmetric and antisymmetric coupled modes, which is a function of wavelength, waveguide geometry and the gap between the two waveguides. Thus, the length of parallel waveguide required in order to fully transfer the optical field from one waveguide to another and back again,  $L_{tot}$ , is given by

$$L_{tot} = \lambda / \delta n_{eff}. \quad (2)$$

With the use of a 2D mode solver (in this case RSOFT FEMSIM), it is therefore possible to determine the theoretically required coupling length in order to split the 1310/1550nm wavelengths while implementing polarisation insensitivity at 1550nm.

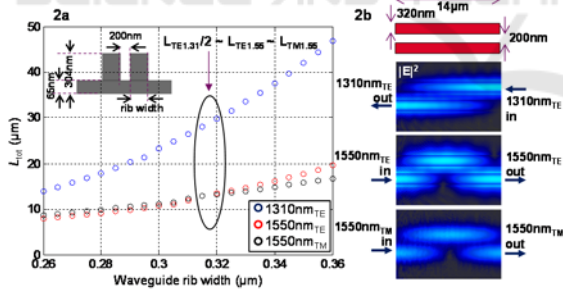


Figure 2a:  $L_{tot}$  versus waveguide rib width. Inset: waveguide geometry in coupling region. Figure 2b: Electrical field intensity plots along the coupling region illustrating the multiplexing mechanism.

Figure 2 shows  $L_{tot}$  as a function of waveguide rib width for a waveguide spacing of 200nm for a 1.31 $\mu$ m TE mode (blue circles), a 1.55 $\mu$ m TE mode (red circles) and 1.55 $\mu$ m TM mode (black circles). The inset in the figure shows the waveguide geometry used. We opted for a ‘rib’ type waveguide with a continuous 65nm slab region for consistency with our standard process, although other waveguide geometries could offer valid starting points. For a

fixed gap between the waveguides of 200nm, the values of  $L_{tot}$  can be obtained as the rib width is varied. In order to satisfy the function defined in figure 1, we require

$$L_{tot}(1.55_{TE}) = L_{tot}(1.55_{TM}) = L_{tot}(1.31_{TE})/2. \quad (3)$$

When this condition is satisfied, the duplexing functionality of the directional coupler is as illustrated in the electric field intensity plots in figure 2b. This is well approximated for a rib width of 315/320nm, where  $L_{tot}(1.55_{TE}) = 13.0/13.5\mu$ m,  $L_{tot}(1.55_{TM}) = 13.0/13.3\mu$ m and  $L_{tot}(1.31_{TE})/2 = 14.0/14.7\mu$ m.

While the above analysis provides a good starting point for the directional coupler design, in reality, the parallel waveguides must approach one other and separate gradually, so as not to incur unwanted bending losses. The actual design is shown in figure 3a. The waveguides are brought together using a sin-function bend whose minimum bending radius is 11 $\mu$ m. Although the coupling strength between the two waveguides decreases exponentially with the gap between them, the power transfer which occurs in the input and output bent waveguide sections is not negligible and is most simply simulated using 3D-FDTD (RSOFT FULLWAVE).

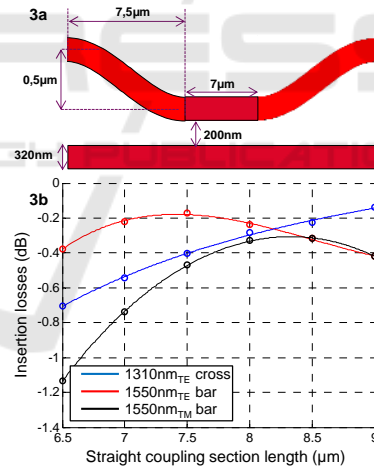


Figure 3a: Implemented directional coupler geometry including input/output S-bends. 3D-FDTD simulated insertion losses (data points in circles, the solid lines are a guide for the eye).

Figure 3 shows the simulated insertion losses for the 1.31 $\mu$ m TE, 1.55 $\mu$ m TE and the 1.55 $\mu$ m TM waveguide modes as a function of the length of the straight coupling section. In order to obtain less than 1dB insertion losses per channel, the FDTD simulations, which included the initial S-bends, revealed that a straight coupling length of between 7 and 9  $\mu$ m is required. This is rather less than the value attained in the simple model

described above, which is due to the significant coupling which takes place in the input/output bent waveguide sections.

### 3 FABRICATION AND TEST

Test structures were fabricated at CEA-LETI on 200mm wafers with a SOI/BOX thickness of 310/800nm. Waveguides were defined using 193nm-DUV lithography and a dry etching process (B. Szlag, 2016).

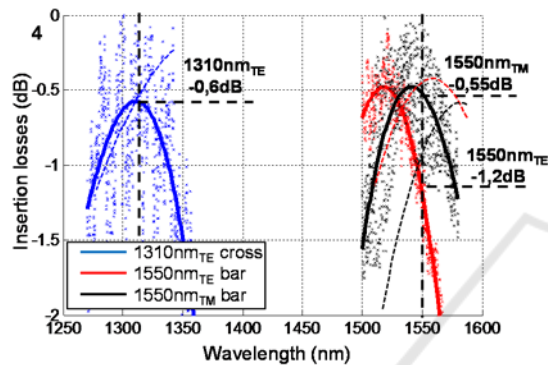


Figure 4: Measured insertion losses of best performing fabricated design variant. Solid lines are fit lines to the data (points), dashed lines are 3D-FDTD simulations of the nominal structure.

Test structures with a range of nominal waveguide widths and coupling section lengths were fabricated. Each variant was triplicated and connected to vertical fibre grating couplers designed to couple 1.31 $\mu$ mTE/1.55 $\mu$ mTE/1.55 $\mu$ mTM light into the waveguides. In order to evaluate the insertion losses for each channel, a reference waveguide was measured with each type of fibre coupler. The ‘cross’ transmission (corresponding to light crossing from one guide to another) and the ‘bar’ transmission (corresponding to light propagation along the same waveguide) of each variant was then measured for each channel. The directional coupler transmission spectra were then obtained by subtracting the corresponding fibre coupler spectra from the directional coupler transmission data.

The transmission spectra of the best performing variant (rib width = 320nm, gap = 200nm, coupling section length = 7 $\mu$ m) are shown in figure 4. The data points are shown as well as polynomial fits (solid lines). The high noise level of the data can be attributed to the summing of the noise in the transmission spectra and the reference spectra. The measured insertion losses for the

1.31 $\mu$ mTE/1.55 $\mu$ mTE/1.55 $\mu$ mTM channels were -0.6/-0.55/-1.2dB. The measured -1dB bandwidth is in the region of 80nm. The use narrowband fibre grating couplers prevented crosstalk measurements, although FDTD simulations show values in the -10 to -15dB range.

For comparison, the 3D-FDTD simulated transmission spectra for this nominal structure are also shown as dashed lines on figure 4. The observed discrepancy as well as the fact that the best performing variant (rib width = 320nm, L = 7 $\mu$ m) was not exactly that identified via FDTD simulation may be firstly attributed to the unsimulated optical coupling in the waveguide routing required to access the test structure and secondly, to departures from the nominal waveguide geometry in the processed devices.

### 4 CONCLUSIONS AND PERSPECTIVES

We have designed, fabricated and measured an integrated silicon low loss O-band/C-band duplexer with polarisation insensitivity at 1550nm. The device shows low measured losses (<1.3dB) at each design wavelength. Further design refinements will likely reduce insertion losses significantly below 1dB, which compares favourably with conventional, discrete optical componentry. Based on this positive result, we are now fabricating a complete circuit, including integrated laser, photodiode and broadband edge coupler to demonstrate the potential of integrated silicon photonics for this application.

### REFERENCES

- L. Vivien, J. Osmond, Jean-Marc Fédéli, Delphine Marris-Morini, Paul Crozat, Jean-François Damlencourt, Eric Cassan, Y. Lecunff, and Suzanne Laval, "42 GHz p.i.n Germanium photodetector integrated in a silicon-on-insulator waveguide," *Opt. Express* 17, 6252-6257 (2009).
- J. Cardenas, C. B. Poitras, K. Luke, L. Luo, P.A. Morton, and M. Lipson. 2014. High Coupling Efficiency Etched Facet Tapers in Silicon Waveguides, *IEEE Photonics Technology Letters*, Vol. 26, No. 23.
- K. Okamoto, 2014. Wavelength-Division Multiplexing Devices in Thin SOI: Advances and Prospects, *IEEE Journal of Selected Topics in Quantum Electronics*, Vol. 20, NO. 4.
- G. Roelkens, D. Van Thourhout, and R. Baets. 2007. Silicon-on-insulator ultra-compact duplexer based on a

- diffractive grating structure. *Opt. Express* 15, 10091-10096.
- J.K. Hong and S.S. Lee. 2007. 1 x 2 Wavelength Multiplexer With High Transmittances Using Extraneous Self-Imaging Phenomenon," *J. Lightwave Technol.* 25, 1264-1268.
- S. Bidnyk, M. Pearson, A. Balakrishnan, M. Gao, D. Feng, H. Liang, W. Qian, C. Kung, J. Fong, P. Zhou, J. Yin, and M. Asghari, 2007. Silicon-on-Insulator Platform for Building Fiber-to-the-Home Transceivers, in *Optical Fiber Communication Conference and Exposition and The National Fiber Optic Engineers Conference*, OSA Technical Digest Series (CD) (Optical Society of America), paper OTuM4.
- B. Szlag ; B. Blampey ; T. Ferrotti ; V. Reboud ; K. Hassan, et al. Multiple wavelength silicon photonic 200 mm R+D platform for 25Gb/s and above applications, 2016. *Proc. SPIE 9891, Silicon Photonics and Photonic Integrated Circuits V*, 98911C (May 13, 2016); doi:10.1117/12.2228744.

